Journal of Constructional Steel Research 140 (2018) 11–24

Contents lists available at ScienceDirect

Journal of Constructional Steel Research

Seismic performance of steel-concrete composite structural walls with prestressed internal bracing

Wenwu Lan [a,b,1], Bing Li [c], Zhongwen Zhang [c,*]

[a] College of Civil Engineering and Architecture, Guangxi University, Nanning 530004, PR China
[b] Guangxi Key Laboratory of Disaster Prevention and Engineering Safety, Guangxi University, Nanning 530004, PR China
[c] School of Civil and Environmental Engineering, Nanyang Technological University, Singapore

ARTICLE INFO

Article history:
Received 14 September 2016
Received in revised form 1 March 2017
Accepted 15 October 2017
Available online xxxx

Keywords:
Steel-concrete composite
Prestress
Internal bracing
Material nonlinearity
Cyclic loading, finite element
Hysteresis loops

ABSTRACT

This paper presents research investigations on the seismic performances of steel-concrete composite structural walls with prestressed internal bracing. The lateral stiffness of the walls was increased with embedded steel while the prestressed internal braces are designed to control the cracks of the wall. Tests are conducted for steel-concrete walls with different arrangement of prestressed internal bracing. The specimens were observed and analyzed by the cracking process and patterns, the hysteresis response, the deformation component and the loss of the prestress during the loading process. Additionally, numerical investigations were performed for the tested specimens. Finite element models were built for these walls.

1. Introduction

Structural walls are critical in resisting lateral load. Designed to resist most or all the lateral loads imposed to the building, their seismic performances are crucial to the seismic performances of the buildings. The seismic behavior of reinforced concrete (RC) structural walls has been extensively investigated over the past decades ([13,14,16–18,20,21,23,24,26,29]). These wall tests have led the development of the current guidelines for seismic design of structural RC walls. For high-rise buildings, the steel-concrete composite walls are sometimes adopted for further increase of the lateral stiffness. There are different types of steel-concrete composite walls. Wright and Gallocher [28] and Wright [27] investigated behavior of the composite wall made of steel plating with infill of concrete. Emori [7] conducted compression and shear test on concrete filled steel box walls. There are also some research investigations conducted about the RC walls with encased shape steel in the section. These investigations include the research conducted by Dan et al. [4,5] and by Lan et al. [11,12] about walls with encased shape steel. There exist more investigations on the columns with encased shape steel including the research conducted by [15], Shanmugam and Lakshmi [22], and Furlong [8]. These research investigations found that the composite RC members with encased shape steel can provide significant lateral strength and stiffness while having good deformation capacity [4,5]. The steel core was found to provide a significant residual strength after crushing of the surrounding concrete (Munoz and Hsu [15]). In designing these members, researchers Munoz and Hsu [15] and Shanmugam and Lakshmi [22] often found an assumption of the perfect bond between the concrete section and the embedded shape steel acceptable. Design codes are available for the steel-concrete composite members [1,3]. Nevertheless, the research investigations concerning the seismic behavior of the composite walls with encased shape steel are very sparse [4].

This paper aims to investigate the seismic behavior a particular composite structural wall which is reinforced by the prestressed internal braces. This structural form can be found in bridge piers as well as some precast buildings. These walls are composite walls with reinforced concrete wall body and encased shape steel. Different forms of prestressed internal bracings can be installed for cracking control or connecting with other structures. Five specimens were tested with different types and arrangements of prestressed braces. The experimental results are presented and discussed in terms of the cracking process and patterns, the hysteresis response, the deformation component and the loss of the prestress during the loading process. Additionally, finite

* Corresponding author.
E-mail address: zwzhang@ntu.edu.sg (Z. Zhang).
[1] Deceased 10 December 2016.

https://doi.org/10.1016/j.jcsr.2017.10.019
0143-974X/

element (FE) models were built for the tested specimens. These models were further adopted to establish parametric studies on the influences of the prestressed bracing for steel-concrete walls with different design parameters.

2. Test program

The aim of the paper is to investigate the influence of the prestressed bracing on the seismic behavior of the steel-concrete composite walls. For this purpose, five specimens were built and tested. All specimens have similar dimensions, reinforcing details and embedded steel. The first specimen is without the prestressed internal bracing while the other four specimens have different types of internal bracing. Details of the experimental program are given in this section.

2.1. Details of specimens

The experimental program includes testing of five specimens named as SW1, SW2, SW3, SW4 and SW5. The specimens have similar geometric dimensions and encased steel as shown in Figs. 1, 2 and Table 1. The variable in these specimens is the existence and the arrangement of the prestressed bracing. SW1 does not include any prestressed bracing. SW2 and SW3 are reinforced with X-shaped bracing running from base to top of the wall as shown in Fig. 2 and Fig. 3. The prestressed bracing are made of two 20 mm threaded tension rods. The rods were installed in polyvinyl chloride (PVC) tube casted together with the wall to reduce the fiction forces between the wall body. Fasteners and nuts were used at the two ends of the tension rods. The tension rods were connected with the wall body by the steel plate welded with the steel cages in the wall. Details of SW2 and SW3 were similar while different post-tension forces were applied to the tension rods as shown in Table 1. SW4 has similar arrangement of threaded tension rods. Instead of PVC tubes, the tension rods of SW4 were installed inside 40 × 30 × 3 rectangular steel tubes. These tubes are expected to work together with the tension cables as the internal bracing. The internal braces in SW5 take different forms. The bracing in this wall is made of two horizontal tension rods at the height of 200 mm and 650 mm above the base, respectively. The tension rods were installed inside two steel tubes casted together with the wall. To distinguish the influence of the tension rods with the contribution of the steel tubes, the steel tubes were discontinuous in the middle of the wall.

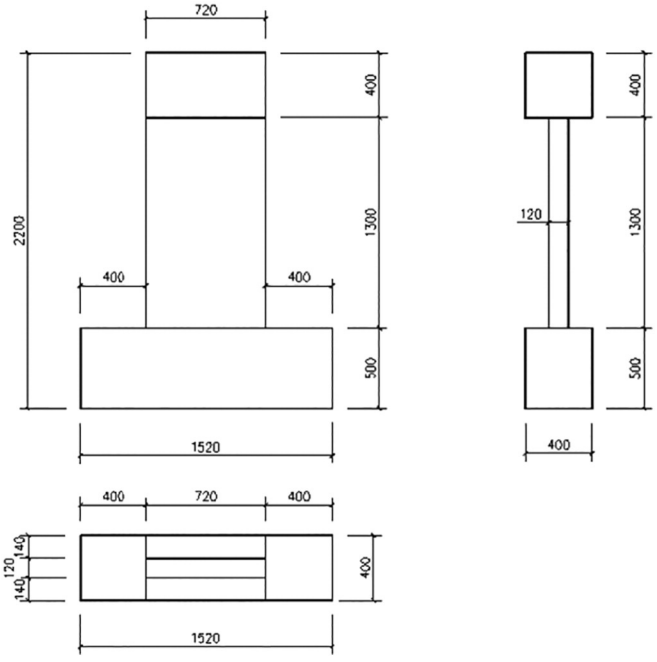

Fig. 1. Specimen dimension.

2.2. Material properties

The strength of the concrete for the tested specimens was derived based on six 150 mm × 150 mm × 150 mm cube samples under similar curing condition and time with the specimens tested. The tested compressive strength ranges from 49.7 MPa to 62.4 MPa. The average compressive strength is 53 MPa and the standard deviation of the tested strength is 5.25 MPa. The maximum nominal aggregate size used in the concrete is 20 mm. The yielding and ultimate strength for the reinforcing bars, shape steel and prestressed bracing are given in Table 2.

2.3. Instrumentation

Strain gauges and transducers were installed in different locations of the wall. Lateral displacement of the wall was measured by the LVDTs at top of the wall. LVDTs were mounted on bodies of the walls to measure the deformation components as shown in Fig. 4. The lateral and axial loads of the wall were measured at the horizontal and vertical jack. Additionally, load cells were mounted at the end of the threaded post-tension rod to measure the change of the tension forces in the rod during the test process.

2.4. Test setup

The test specimens were attached to a loading apparatus enabling the walls to go through single-curvature bending as demonstrated in Fig. 4. The axial load was applied to the wall by the vertical jack attached to the loading frame. Rollers were installed below the jack to ensure the free rotating boundary condition and steel loading frame was installed to distribute the axial load. The lateral load was applied by a horizontal actuator connected with the reaction wall and the test specimens by pins. The bottom of the wall was connected to laboratory strong floor by prestressing rods, which aimed to prevent horizontal movement between wall base and the strong floor as well as the overturning movement. The post-tension forces applied to the wall were applied though jacks at the ends of the wall as shown in Fig. 2.

In the experimental tests, the axial load was applied before the post-tension forces and the lateral loads. For all specimens, a constant axial load was applied and kept during the entire experimental process. The post-tension forces for the threaded rods were applied before the lateral load was applied. The tension forces were controlled by the load cells. After the load was applied, the nuts were fastened and the tension force was not adjusted afterward even the post-tension force may lose due to various reasons in the experiments. The lateral load of the wall divides into two stages. The peak lateral load of the first load cycle was 20 kN for both the negative and the positive loading direction. Following which the peak lateral load increased by 20 kN for each level in the following load reversals until the wall yields. After the wall yielded as detected by the attached strain gauges, the lateral load of the specimens was controlled by maximum displacements as multiples of 3.83 mm which is the estimated first yield lateral displacement for SW1. Each level of cyclic lateral load cycle repeated three times before they next level of lateral load was applied as shown in Fig. 5. The lateral load terminated when the lateral load capacity of the wall reduced to less than 85% of the maximum lateral load.

3. Experimental observations and results

3.1. Cracking pattern and failure mechanisms

Fig. 6 illustrates the cracking patterns of the specimens at the final loading stage. For all specimens, the cracks were developed in generally similar patterns. The first cracks were found at lateral displacement of